Journal of Photochemistry and Photobiology A: Chemistry 271 (2013) 45–55

Contents lists available at ScienceDirect

Journal of Photochemistry and Photobiology A: Chemistry

journal homepage: www.elsevier.com/locate/jphotochem

Photocatalytic decompositions of methanol and ethanol on Au supported by pure or N-doped TiO_2

Andrea Gazsi, Gábor Schubert, Tamás Bánsági, Frigyes Solymosi*

MTA-SZTE Reaction Kinetics and Surface Chemistry Research Group, Rerrich Béla tér 1, H-6720 Szeged, Hungary

ARTICLE INFO

Article history:
Received 6 June 2013
Received in revised form 16 July 2013
Accepted 6 August 2013
Available online xxx

Keywords:
Methyl alcohol
Ethyl alcohol
Methyl formate
Photolysis
Au/TiO_2 catalyst
Effect of N-doping

ABSTRACT

The effects of Au particles of different sizes were investigated on the photocatalytic decompositions of methanol and ethanol on pure or N-doped TiO_2. IR studies revealed that the deposition of Au promoted the dissociation of both compounds during illumination and also resulted in the formation of formate species. Whereas the photo-induced decompositions of methanol and ethanol occurred to only a limited extent on pure TiO_2, the deposition of Au, particularly as nanosized particles, markedly enhanced the rate and the extent of the photocatalyzed reactions. An interesting feature of the photodecomposition of methanol was that, besides H_2, CO_2 and CO, a significant amount of methyl formate was also produced. Addition of H_2O or O_2 to the alcohol in both cases decreased the level of CO formed, and in the case of methanol CO was completely eliminated. Au particles on N-doped TiO_2 with a lower bandgap catalyzed the photodecompositions of both compounds even in visible light.

1. Introduction

Following the pioneering work of Haruta et al. [1,2], who demonstrated the unexpectedly high catalytic activity of nanosized supported Au particles, great efforts have been made to exploit this property of Au in several areas of catalysis [3–5]. As the generation of H_2 free of CO is one of the challenges in heterogeneous catalysis, the catalytic behavior of Au has also been tested from this aspect. It was found that supported Au particles effectively catalyze the production of H_2 in the thermal decompositions of HCOOH [6–10], CH_3OH [11–18], C_2H_5OH [19–23] and CH_3OCH_3 [24] at 423–573 K. Pure, CO-free H_2 was obtained, but only in the catalytic decomposition of HCOOH at higher temperatures [6–8]. A further development in this topic was the production of H_2 by photocatalytic decomposition of the above compounds over supported Au samples at room temperature [25–32]. In the continuation of this research program in the present work we investigated the photocatalytic decompositions of CH_3OH and C_2H_5OH on various Au/TiO_2 catalysts. The overall aim is to elaborate experimental conditions for the generation of H_2 with the lowest achievable CO content, to identify surface species formed in the photoreaction and to produce H_2 in visible light by narrowing the bandgap of TiO_2 by N-doping. The development of an effective photocatalyst using visible light is a challenging project, as visible light accounts for 50% of total solar energy in contrast to UV light, which accounts only ~5% of total solar energy.

2. Experimental

2.1. Materials and preparation of the catalysts

The following compounds were used as supports. TiO_2 (Hombikat, 200 m^2/g and P25, 51 m^2/g), SiO_2 (CAB-O-SiL, 198 m^2/g). Supported Au catalysts with an Au loading of 1, 2 or 5 wt% were prepared by a deposition-precipitation method. $HAuCl_4 \cdot aq$ (p.a., 49% Au, Fluka AG) was first dissolved in triply distilled water. After the pH of the aqueous $HAuCl_4$ solution had been adjusted to 7.5 by the addition of 1 M NaOH solution, a suspension was prepared with the finely powdered oxidic support, and the system was kept at 343 K for 1 h under continuous stirring. The suspension was then aged for 24 h at room temperature, washed repeatedly with distilled water, dried at 353 K and calcined in air at 573 K for 4 h. 1% Au/TiO_2 was also purchased from STREM Chem. Inc. This sample is marked "Aurolite". For the preparation of N-doped TiO_2 we applied the description of Xu et al. [33]. Titanium tetrachloride was used as a precursor. After several steps the NH_3-treated TiO_2 slurry was vacuum dried at 353 K for 12 h, followed by calcination at 723 K in flowing air for 3 h. This sample is noted with "SX".

The sizes of the Au nanoparticles were determined with an electron microscope. We obtained the following values: 1.5–2.0 nm for 1% Au/TiO_2 (Aurolite), 10–15 nm for 1% Au/TiO_2 (Hombi) and 6.0–7.0 nm for 1% Au/SiO_2 (Cabosil). For photocatalytic

* Corresponding author. Tel.: +36 62544107; fax: +36 62 544 106.
E-mail address: fsolym@chem.u-szeged.hu (F. Solymosi).

1010-6030/$ – see front matter © 2013 Published by Elsevier B.V.
http://dx.doi.org/10.1016/j.jphotochem.2013.08.009

measurements the sample (70–80 mg) was sprayed onto the outer side of the inner tube from aqueous suspension. The surface of the catalyst film was 168 cm^2. The catalysts were oxidized at 573 K and reduced at 573 K in situ.

For IR studies the dried samples were pressed in self-supporting wafers (30 mm × 10 mm ~10 mg/cm^2). For photocatalytic measurements the sample (70–80 mg) was sprayed onto the outer side of the inner tube from aqueous suspension. For photocatalytic studies the sample was sprayed onto the outer side of the inner tube from aqueous suspension. The surface of the catalyst film was 168 cm^2. The catalysts were oxidized at 573 K and reduced at 573 K in the IR cell or in the catalytic reactor for 1 h. Methanol and ethanol were the products of Scharlau with purity of 99.98 and 99.7%, respectively.

2.2. Methods

For the determination of bandgap of solids, we applied the same procedures as described in previous papers [34,35]. Diffuse reflectance spectra of TiO_2 samples were obtained using an UV/Vis spectrophotometer (OCEAN OPTICS, Typ.USB 2000) equipped with a diffuse reflectance accessory. In the calculation we followed the procedure of Beranek and Kisch [34], who used the equation $\alpha = A(h\nu - E_g)^n/h\nu$, where α is the absorption coefficient, A is a constant, $h\nu$ is the energy of light, and n is a constant depending on the nature of the electron transition. Assuming an indirect bandgap ($n = 2$) for TiO_2, with α proportional to $F(R_\infty)$, the bandgap energy can be obtained from the plots of $[F(R_\infty)h\nu]^{1/2}$ vs. $h\nu$, as the intercept at $[F(R_\infty)h\nu]^{1/2} = 0$ of the extrapolated linear part of the plot.

Table 1
Some characteristic data for pure and N-modified TiO2.

Sample	Pretreatment temperature (K)	Surface area (m^2/g)	Band gap (eV)	Notation
TiO_2	As received	200	3.17	Hombikat
TiO_2	723	135		
TiO_2	723	265	3.00	SX
TiO_2 + N	723	79	1.96	

The surface area of the catalysts were determined by BET method with N_2 adsorption at ~100 K. Data are listed in Table 1.

Photocatalytic reaction was followed in the same way as described in our previous paper [35]. Briefly the photoreactor (volume: 970 ml) consists of two concentric Pyrex glass tubes fitted one into the other and a centrally positioned lamp. It is connected to a gas-mixing unit serving for the adjustment of the composition of the gas or vapor mixtures to be photolyzed in situ. The length of the concentric tubes was 250 mm. The diameter of outer tube was 70 mm, and that of the inside tube 28 mm long. The width of annulus between them was 42 mm, and that of the photocatalyst film was 89 mm. We used a 15 W germicide lamp (type GCL 307T5L/CELL, Lighttech Ltd., Hungary), which emits predominantly in the wavelength range of 250–440 nm, its maximum intensity is at 254 nm. For the visible photocatalytic experiments another type of lamp was used (Lighttech GCL 307T5L/GOLD) with 400–640 nm wavelength range and two maximum intensities at 453 and 545 nm. The approximate light intensity at the catalyst films are 3.9 mW/cm^2 for the germicide lamp and 2.1 mW/cm^2 for the other lamp. The incident light intensities were determined by

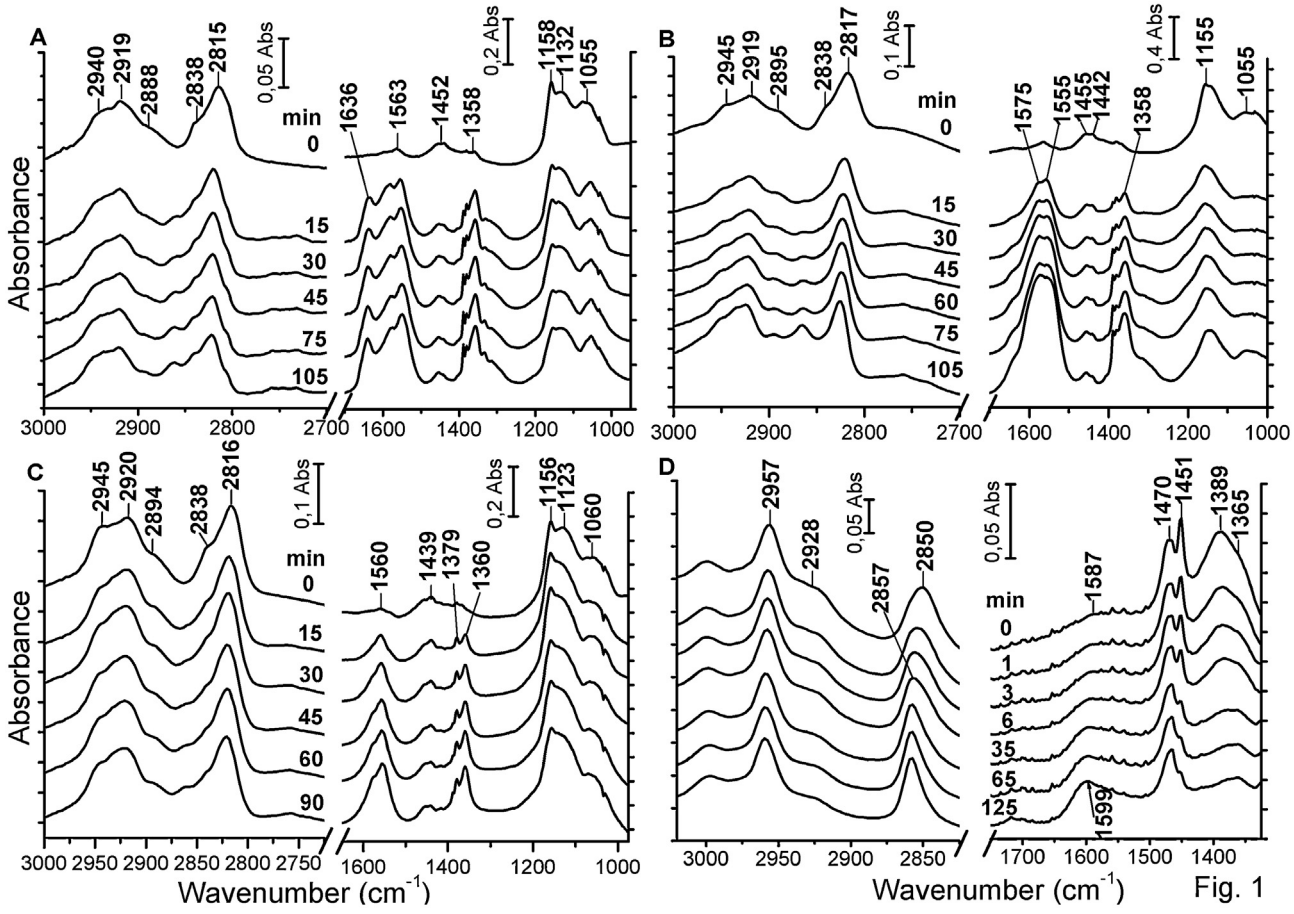

Fig. 1. Effects of illumination time on the FTIR spectra of adsorbed CH_3OH on 1% Au/TiO_2 (Aurolite) (A), 1% Au/TiO_2 (Hombikat) (B), TiO_2 (P25) (C) and 1% Au/SiO_2 (D).

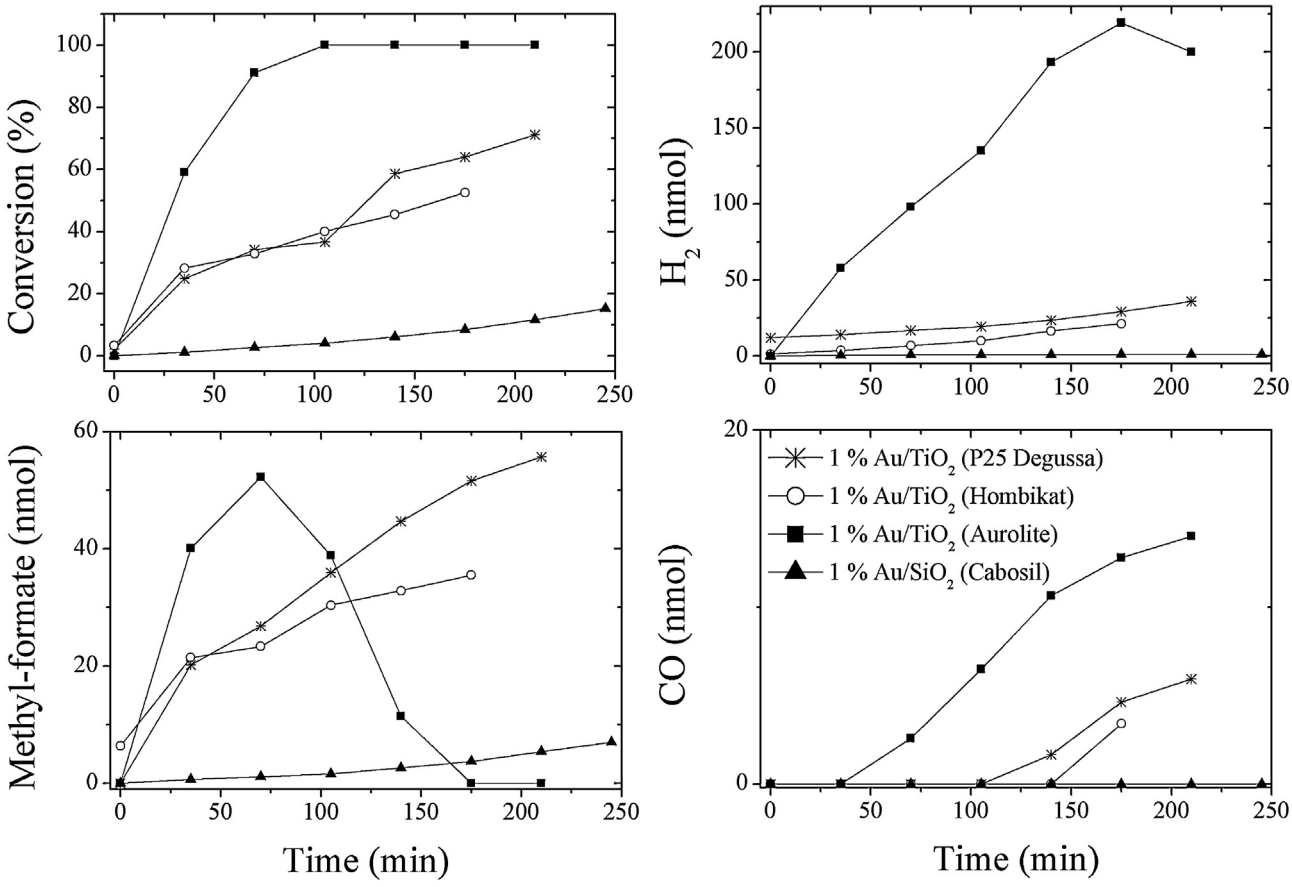

Fig. 2. Photocatalytic decomposition of CH_3OH on 1% Au/TiO_2 and 1% Au/SiO_2 samples.

an actionometry. Methanol (~1.2%, 227 μmol) and ethanol (~1.3%, 252 μmol) were introduced in the reactor through an externally heated tube avoiding condensation. The carrier gas was Ar, which was bubbled through alcohols at room temperature. The gas-mixture was circulated by a pump. The reaction products were analyzed with a HP 5890 gas chromatograph equipped with PORAPAK Q and PORAPAK S packed columns. The sampling loop of the GC was 500 μl. The amount of all products were related to this loop.

For infrared (IR) studies a mobile IR cell housed in a metal chamber was used. The sample can be heated and cooled in situ. The IR cell can be evacuated to 10^{-5} Torr using a turbo molecular pumping system. The samples were illuminated by the full arc of a Hg lamp (LPS-220, PTI) outside the IR sample compartment. The IR range of the light was filtered by a quartz tube (10 cm length) filled with triply distilled water applied at the exit of the lamp. The filtered light passed through a high-purity CaF_2 window into the cell. The light of the lamp was focused onto the sample. The output produced by this setting was 300 mW cm^{-2} at a focus of 35 cm. The maximum photon energy at the sample is ca. 5.4 eV. After illumination, the IR cell was moved to its regular position in the IR beam. Infrared spectra were recorded with a Biorad (Digilab. Div. FTS 155) instrument with a wavenumber accuracy of ±4 cm^{-1}. All the spectra presented in this study are difference spectra.

3. Results and discussion

3.1. Adsorption and reactions of methanol

The adsorption of CH_3OH on Au/TiO_2 (Aurolite) at 300 K produced absorption bands at 2940, 2919, 2888, 2838 and 2815 cm^{-1} in the high-frequency range, and at ~1563, 1452, ~1358, 1158, 1132 and 1055 cm^{-1} in the low-frequency region (Fig. 1A). Illumination of the CH_3OH vapor catalyst system resulted in only slight attenuation in the high-frequency range, but led to a significant intensification of the very weak bands at 1563 and 1358 cm^{-1}. In light of the IR spectroscopic results of previous studies [16,30,35,36], the bands at 2940 and ~2838 cm^{-1} can be assigned to the asymmetric and symmetric stretching frequencies of adsorbed CH_3OH and those at ~2919 and ~2815 cm^{-1} to adsorbed methoxy (CH_3O). The peaks in the interval 1000–1200 cm^{-1} are due to the C—O stretching of the two adsorbed species. Approximately, same features were registered for Au/TiO_2 (Hombi) sample (Fig. 1B). Accordingly, the occurrence of the following steps may be presumed:

$$CH_3OH_{(g)} = CH_3OH_{(a)} \quad (1)$$

$$CH_3OH_{(a)} = CH_3O_{(a)} + H_{(a)} \quad (2)$$

The appearance of new absorption bands at 1563 and 1358 cm^{-1} suggests that adsorbed formate species are also formed during the photolysis [35,36]. With regard to the results of photocatalytic studies (next chapter), adsorbed formate is very probably formed in the dissociation of $HCOOCH_3$ (methyl formate) produced by the photoconversion of CH_3OH [30–32]. Similarly to HCOOH, $HCOOCH_3$ does not exhibit a vibration at 1558–1578 cm^{-1} [31,32]. As nearly the same spectral features were observed for the pure TiO_2 (P25) sample (Fig. 1C), it may be concluded that all these species locate on the TiO_2 surface.

We obtained different results on Au/SiO_2. Following the adsorption of CH_3OH, absorption bands at ~2957, ~2850, 1470, 1451 and 1389 cm^{-1} predominated in the spectrum, indicating that CH_3OH is mainly adsorbed molecularly on this catalyst. Illumination exerted

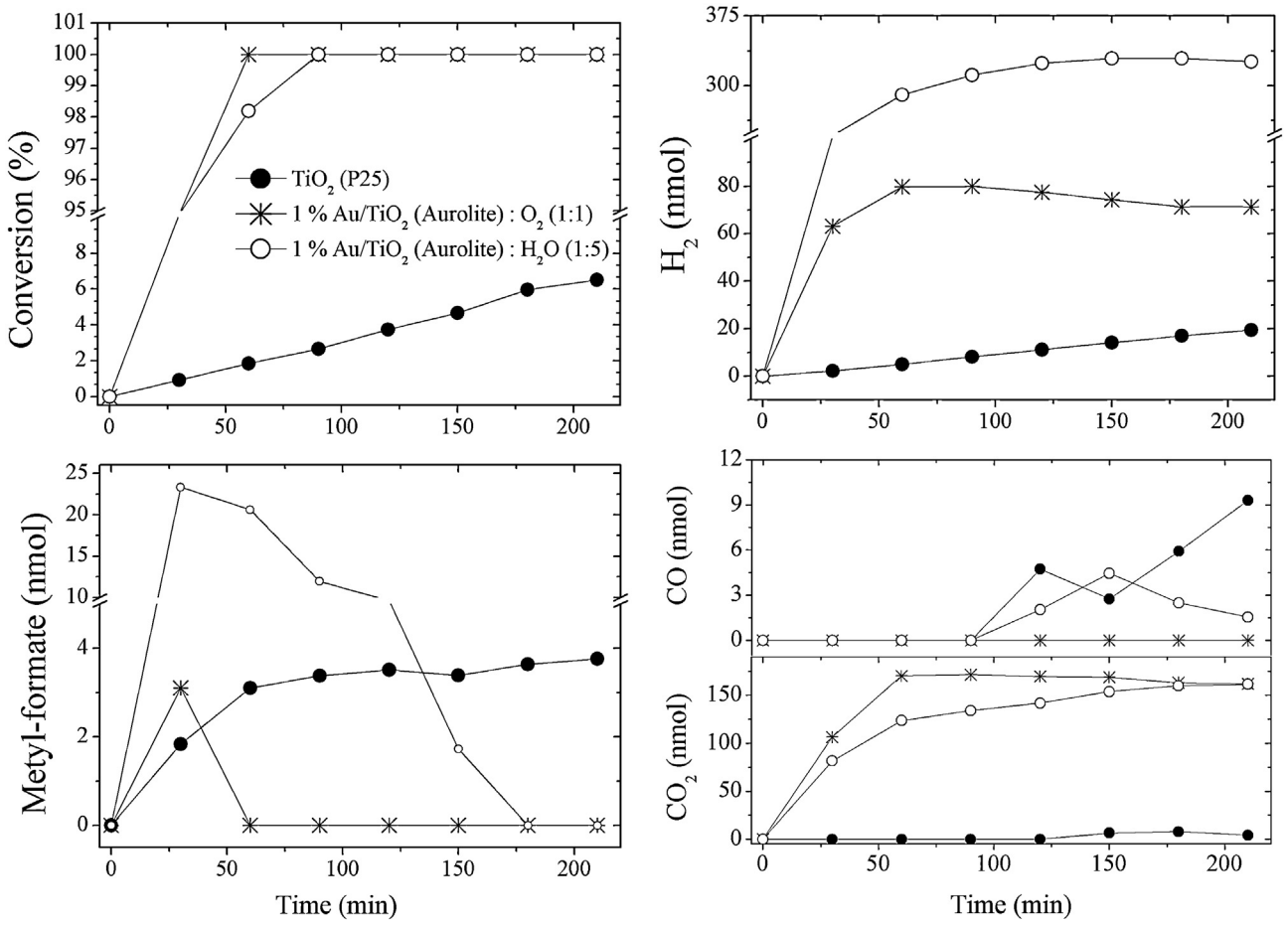

Fig. 3. Effects of H_2O and O_2 addition on the photocatalytic decomposition of CH_3OH over 1% Au/TiO_2 (Aurolite) catalyst.

only very slight alterations in the IR spectrum. However, the very weak absorption at around 1587 cm^{-1}, due to the asymmetric stretch of formate, was clearly strengthened. IR spectra are shown in Fig. 1D. As no formate species exists on SiO_2, it follows that a proportion of the processes involved occur on the Au particles.

Fig. 2 depicts the conversion of CH_3OH and the formation of various products on different Au/TiO_2 catalysts as a function of the duration of illumination. The most effective catalyst was clearly 1% Au/TiO_2 (Aurolite), on which almost complete photodecomposition of the CH_3OH was attained in ~100 min. The main products were H_2 and $HCOOCH_3$: CO and CO_2 were formed in only relatively small amounts. When CH_3OH has been completely decomposed, the amount of $HCOOCH_3$ started decreasing. At the same time CO appeared in the products. As reported previously [30], the photocatalytic decomposition of CH_3OH also occurs on pure TiO_2 (Hombi): the conversion of CH_3OH reached only 2–3% in 240 min. As the photoactivity of pure TiO_2 depends on its origin, for the reliable establishment of the effects of Au we examined the photocatalytic decomposition of CH_3OH on the same TiO_2 (P25) as used for the preparation of Au/TiO_2 (Aurolite). The activity of this TiO_2 (P25) was higher than that of TiO_2 (Hombi), but even on this sample the extent of photodecomposition of CH_3OH reached only 6–7% in 210 min (Fig. 3). Note that methyl formate was also produced on this TiO_2. In order to assess the importance of the TiO_2 support and that of the metal/TiO_2 contact, the photolysis of CH_3OH was also carried out on a 2% Au/SiO_2 catalyst. As can be seen in Fig. 2, only slight decomposition occurred; the conversion approached 15% in 240 min.

A great effort was made to eliminate or fundamentally reduce the formation of CO. The addition of H_2O to the CH_3OH (a H_2O/CH_3OH ratio of 5:1) enhanced the production of H_2 and completely eliminated the CO from the products during the completion of reaction, ~90 min and even decreased the CO content afterwards (Fig. 3). Similar results were found when O_2 was added to the CH_3OH. At an O_2/CH_3OH ratio of 1:1, the formation of CO ceased completely. At the same time, the production of H_2 and $HCOOCH_3$ also decreased, while the amount of CO_2 generated increased. This clearly indicates the oxidation of CH_3OH and/or the products. The main results of the effects of H_2O and O_2 are presented in Table 2.

The effects of N incorporation into TiO_2 were examined by using the TiO_2 (SX) sample, which was considerably less active than the Au/TiO_2/Aurolite. As shown in Fig. 4, the photoactivity of Au/TiO_2 (SX) was enhanced significantly by N-doping. When the photolysis was performed in visible light, the extent of photodecomposition was lower, but the positive effect of N-doping was clearly exhibited (Fig. 5).

For comparison, we studied the thermal decomposition of CH_3OH on the most active Au/TiO_2 (Aurolite) catalyst. No decomposition was observed at 300–423 K in 60 min. The decomposition started at 448 K, and reached ~3% in 60 min. It is important to point out that no $HCOOCH_3$ was formed in the thermal reaction.

In the interpretation of the effects of illumination, it should be taken into account that the rate-determining step in the thermal decomposition of CH_3OH is the cleavage of one of the C—H bonds in the adsorbed CH_3O species. The occurrence of this step on TiO_2 at 300 K requires activation, as otherwise no reactions occur at all.

Table 2
Effect of H_2O and O_2 addition on the photocatalytic decomposition of methanol and ethanol on 1% Au/TiO_2 (Aurolite).

	Conversion (%)		CO (%)		CO/H_2 ratio	
	60 min	180 min	60 min	180 min	60 min	180 min
CH_3OH	91.1	100	1.5	3.9	0.03	0.07
H_2O/CH_3OH (5:1)	98.2	100	0	0.5	0	0.007
O_2/CH_3OH (1:1)	100	100	0	0	0	0
C_2H_5OH	100	100	6.1	11.9	0.16	0.3
H_2O/C_2H_5OH (5:1)	96.8	100	1.9	4.3	0.05	0.08
O_2/C_2H_5OH (1:1)	100	100	2.0	3.6	0.09	0.1

Illumination, however, initiated the decomposition of this surface species even on pure TiO_2 at 300 K, which can be explained by the donation of photoelectrons formed in the photo-excitation process

$$TiO_2 + h\nu = h^+ + e^- \quad (3)$$

to the CH_3O species:

$$CH_3O_{(a)} + e^- = CH_3O_{(a)}{}^{\delta-} \quad (4)$$

which decomposes to H_2 and CO:

$$CH_3O_{(a)}{}^{\delta-} = CH_2O_{(a)}{}^{\delta-} + H_{(a)} \quad (5)$$

$$CH_2O_{(a)}{}^{\delta-} = CO_{(g)}{}^{\delta-} + H_{2(g)} \quad (6)$$

However, even the photo-induced reaction occurred to only a very limited extent on pure TiO_2, a finding which can be attributed to the fast recombination of the electrons and holes formed in the photo-excitation process. The incorporation of N into the TiO_2 appreciably increased the extent of photodecomposition, very likely as a consequence of the prevention of electron-hole recombination [30–32]. The deposition of Au onto TiO_2 greatly improved the photocatalytic effect of the TiO_2. We assume that the CH_3O species formed on the Au particles or at the Au/TiO_2 interface are much more reactive than that located on TiO_2.

An interesting feature of the photocatalytic decomposition of methanol is the formation of methyl formate. This compound has been considered as a precursor in the synthesis of formamide, dimethyl formamide, acetic acid, propionic acid, cyanhydric acid and several other materials [37]. It is mainly synthesized by dehydrogenation of methanol over Cu-based catalyst at higher temperatures. However, recent works showed that it is also formed in the photocatalytic oxidation [38–41] and decomposition of methanol on polycrystalline TiO_2 at room temperature [30].

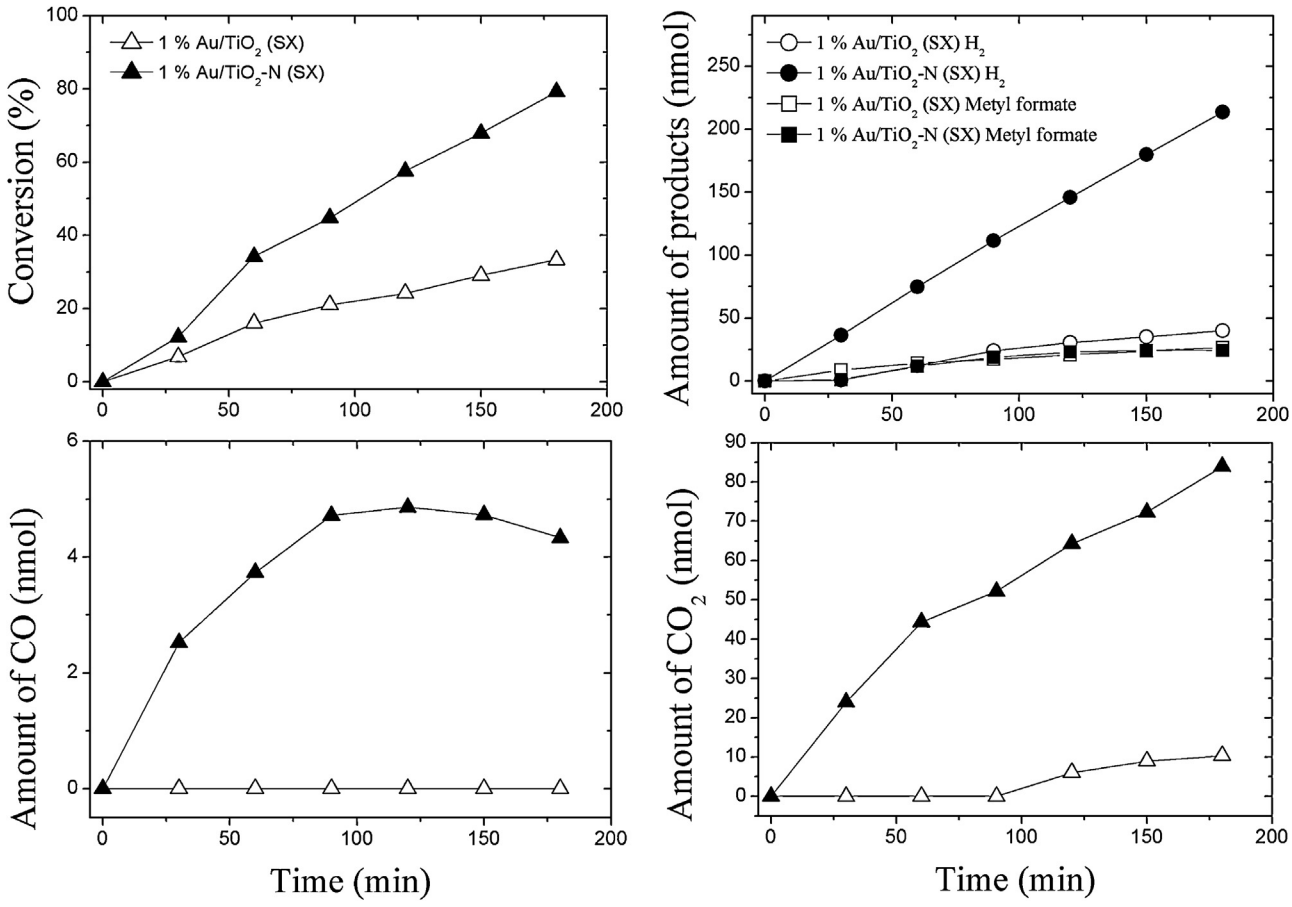

Fig. 4. Effects of N doping of TiO_2 (SX) on the photocatalytic decomposition of CH_3OH on 1% Au/TiO_2 and 1% Au/TiO_2 + N.

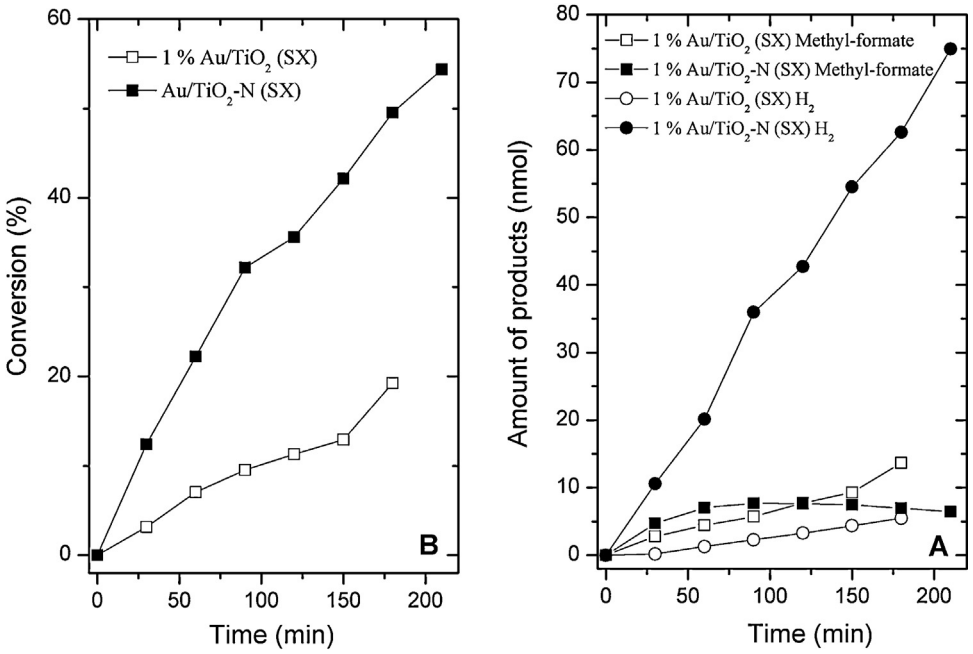

Fig. 5. Effects of N doping of TiO_2 (SX) on the photocatalytic decomposition of CH_3OH in the visible light. 1% Au/TiO_2 (A) and 1% Au/TiO_2 + N (B).

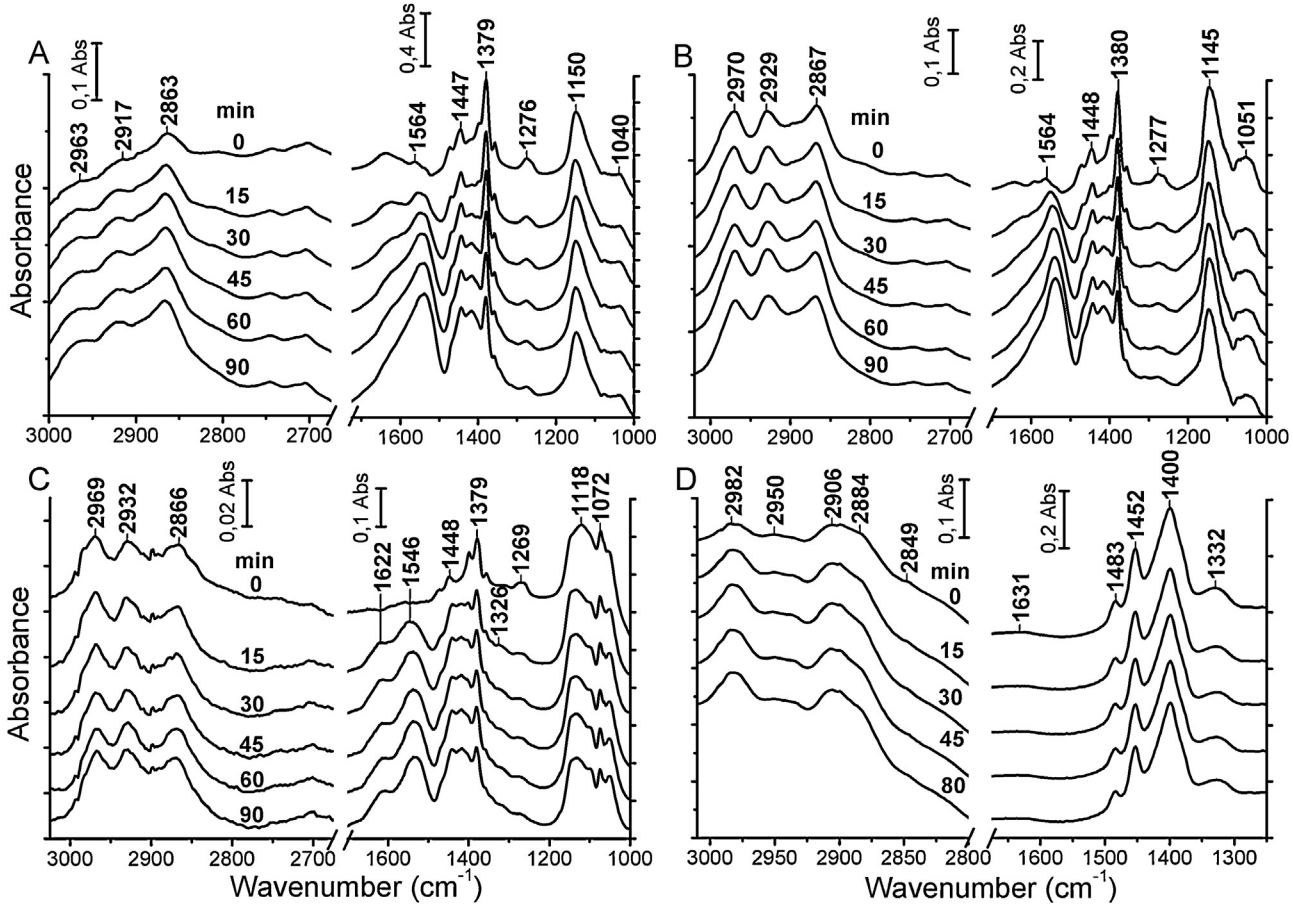

Fig. 6. Effects of illumination time on the FTIR spectra of adsorbed C_2H_5OH on TiO_2 (P25) (A), 1% Au/TiO_2 (Hombikat) (B), 1% Au/TiO_2 (Aurolite) (C) and 1% Au/SiO_2 (D).

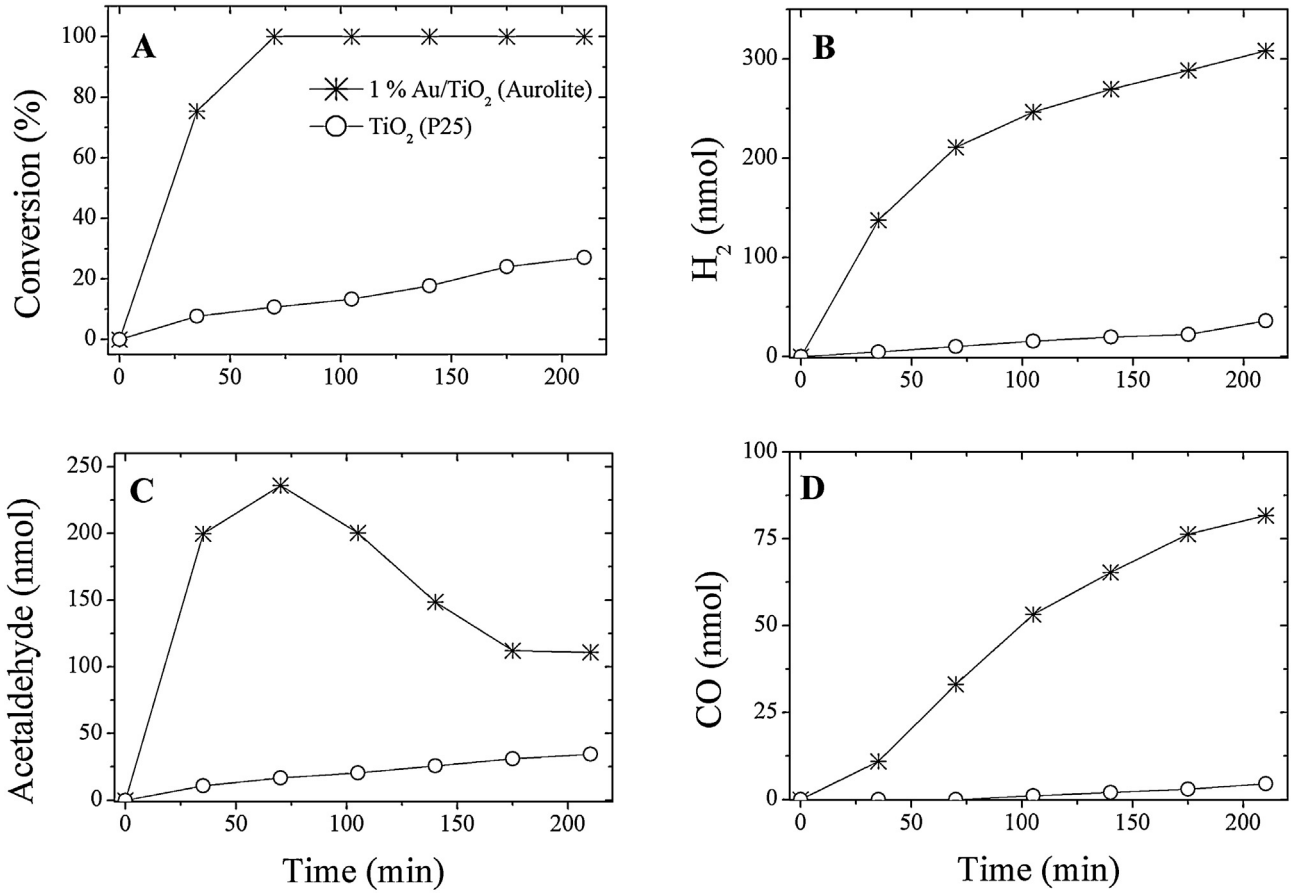

Fig. 7. Photocatalytic decomposition of C_2H_5OH on 1% Au/TiO_2 (Aurolite) and TiO_2 (P25) samples.

Its production was markedly increased when Pt metals were deposited on TiO_2 [30]. The highest yield of methyl formate was measured for Pt/TiO_2 (62.2) and the lowest one for Ru/TiO_2 (26.0). The CO/H_2 ratio varied between 0.017 and 0.023. Au nanoparticles also enhanced the production of methyl formate (Fig. 2). The yield of methyl formate on the most active Au/TiO_2 (Aurolite) was 78.0 at the maximum (60 min). The formation of $HCOOCH_3$ can be ascribed to the recombination of CH_2O formed in the process of CH_3O dissociation (Eq. (4) and (5)):

$$2CH_2O_{(a)} = HCOOCH_{3(a)} \quad (7)$$

or by the reaction of CH_2O with a further CH_3O species:

$$CH_2O_{(a)} + CH_3O_{(a)} = HCOOCH_{3(a)} + H_{(a)} \quad (8)$$

Recent studies performed under UHV conditions on preoxidized TiO_2(1 1 0) disclosed that methyl formate is produced from the photo-oxidation of methanol even at ~200 K [42]. Its formation required that both methoxy and formaldehyde be present on the surface, indicating that the photochemical activation of formaldehyde is faster than the methoxy photooxidation to formaldehyde. In contrast to above reaction steps it was assumed that methyl formate is formed in the coupling of HCO with methoxy species.

The fact that the concentration of $HCOOCH_3$ starts decreasing when CH_3OH almost completely consumed suggests the occurrence of the photocatalytic decomposition of $HCOOCH_3$. This feature appeared only on the most effective Au/TiO_2 (Fig. 2). It was not observed even on the TiO_2-supported Pt metals [30] indicating the exceptionally high reactivity of Au in nanosize on TiO_2. As IR spectra show the presence of adsorbed formate very likely formed in the dissociation of $HCOOCH_3$, its photo-induced decomposition can be described as follows:

$$HCOO_{(a)} + e^- = HCOO_{(a)}{}^{\delta-} \quad (9)$$

$$HCOO_{(a)} = CO_2{}^{\delta-} + H_{(a)} \quad (10)$$

$$CO_2{}^{\delta-} + h^+ = CO_{2(g)} \quad (11)$$

The formation of CO in this stage of photodecomposition (Fig. 2) suggests the occurrence the reaction

$$2HCOO_{(a)}{}^{\delta-} = 2CO_2 + 2OH^{\delta-}{}_{(a)} \quad (12)$$

The promoting effect of Au deposited on TiO_2 can be explained by the better charge carrier separation induced by illumination and by the occurrence of an electronic interaction between the Au particles and n-type TiO_2 [43,44]. The role of the electronic interaction between metals and TiO_2 has been first demonstrated in the catalytic decomposition of formic acid on Ni deposited on pure and doped TiO_2 [45]. As far as we are aware, TiO_2 was first used as a support in this case [45,46]. As the work function of TiO_2 (~4.6 eV) is less than that of Au (5.31 eV), electron transfer is expected to occur from TiO_2 to the deposited Au, which increases the activation of adsorbed molecules. We assume that illumination enhances the extent of electron transfer from TiO_2 to Au at the interface of the two solids, leading to increased decomposition. The Schottky barrier formed at Au and TiO_2 interface can also serve as an efficient barrier preventing electron-hole recombination [28,47,48]. As was pointed out by Li et al. [28] smaller gold particles induce more negative Fermi level shift than the bigger particles. On the

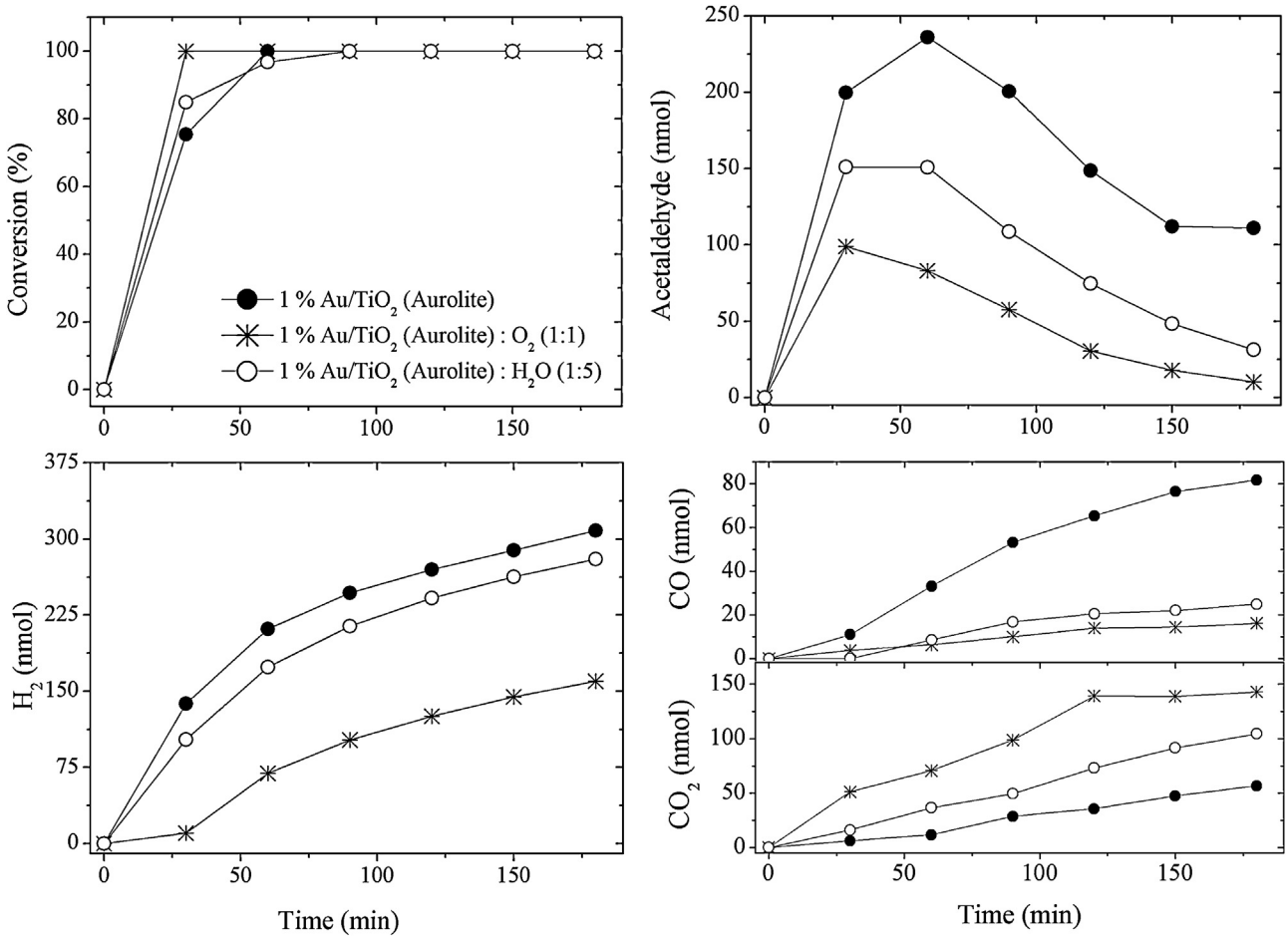

Fig. 8. Effects of H_2O and O_2 addition on the photocatalytic decomposition of C_2H_5OH over 1% Au/TiO_2 (Aurolite) catalyst.

basis of this consideration we expect that the catalyst with smaller gold nanoparticles is catalytically more active than that with larger gold particles.

3.2. Adsorption and reactions of ethanol

In harmony with our previous studies [23], the adsorption of C_2H_5OH on Au/TiO_2 (Aurolite) produced intense absorption bands in the C-H stretching region of the IR spectrum at 2969, 2932 and 2866 cm^{-1} and bands of different intensities at 1448, 1379, 1269, 1118 and ~1072 cm^{-1} (Fig. 6). Virtually identical spectra were measured following the adsorption of C_2H_5OH on the pure TiO_2 and on other Au/TiO_2 samples. In view of the results of previous studies [19,23], the major bands at 2969 and 2866 cm^{-1} can certainly be assigned to the asymmetric and symmetric stretches, and the peaks at 1118 and 1072 cm^{-1} to the ν(OC) vibrations of the ethoxy group. The presence of molecularly adsorbed ethanol is indicated by the absorption band at 1279 cm^{-1}, due to the δ(OH), and at 1379 cm^{-1}, due to $\nu(\delta CH_3)$ of ethanol. Accordingly C_2H_5OH readily dissociates on TiO_2 and Au/TiO_2 even at room temperature without illumination:

$$C_2H_5OH_{(g)} = C_2H_5OH_{(a)} \quad (13)$$

$$C_2H_5OH_{(a)} = C_2H_5O_{(a)} + H_{(a)} \quad (14)$$

As a result of irradiation, the very weak absorption at 1550–1564 cm^{-1} was converted into a well-detectable peak, the intensity of which increased with the duration of illumination. This absorption band is very probably due to the asymmetric stretch of formate species. It should be noted that there was no peak at 1718–1723 cm^{-1} due to CH_3CHO. Absorption bands identified on Au/SiO_2 sample (Fig. 6D) suggest that the dissociation of C_2H_5OH did not occur on this catalyst to detectable extent by IR spectroscopy.

Whereas the conversion of C_2H_5OH on the pure TiO_2 (P25) used for the preparation of Au/TiO_2 (Aurolite) was less than 20% in 60 min, in the presence of 1% Au it was almost 100% (Fig. 7). The primary products were H_2 and CH_3CHO, the amounts of which increased as the duration of illumination was lengthened. When the total conversion of the C_2H_5OH was attained, the concentration of CH_3CHO decreased, indicating the occurrence of its photo-induced degradation (Fig. 7). In the case of TiO_2 (Hombikat) we examined the effect of Au loading on the photocatalytic decomposition of ethanol. The extent of the conversion is gradually increased with the rise of Au content from ~20% (pure TiO_2) to ~100% on 5% Au/TiO_2 in 210 min. The formation of CO in the photocatalytic decomposition of C_2H_5OH was more extensive than in the photoreaction of CH_3OH. The addition of H_2O to the C_2H_5OH exerted only slight effect on the conversion, but markedly lowered the CO content on the Au/TiO_2 (Aurolite) catalyst (Fig. 8). At a H_2O/C_2H_5OH ratio of 5:1, the amount of CO decreased from 6.1% to 1.9%, and the CO/H_2 ratio from 0.16 to 0.05 at 60 min. The quantity of CH_3CHO also decreased. The addition of O_2 to the C_2H_5OH also led to lower amounts of all products, with the exception of CO_2. At an O_2/CH_3OH ratio of 1:1, the formation of CO decreased to 2.0%, and the CO/H_2 ratio to 0.09%. In this case the photo-oxidation of C_2H_5OH is to be expected. Some characteristic data are presented in Table 2.

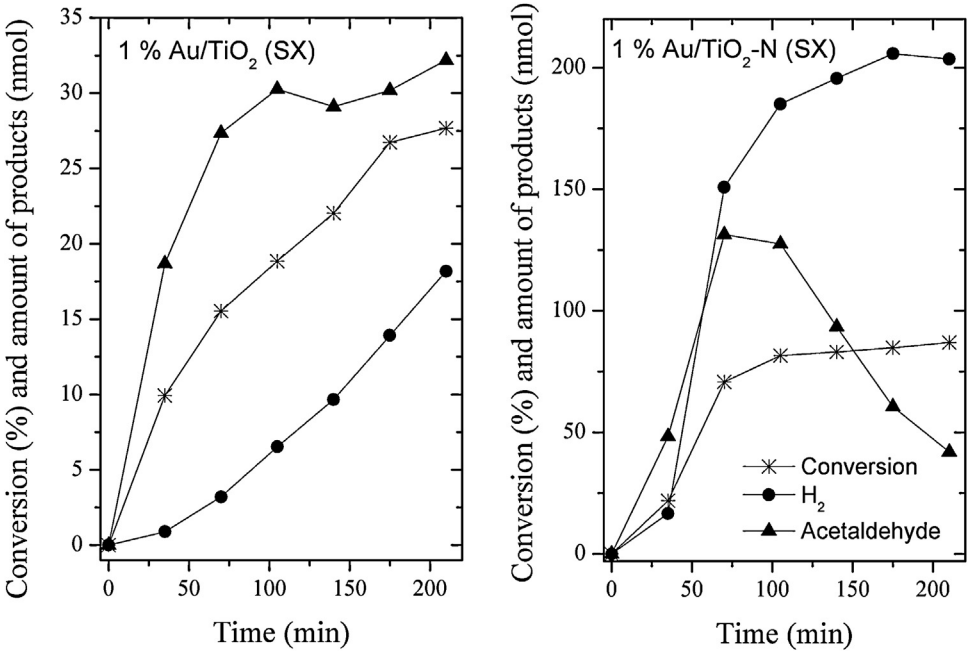

Fig. 9. Effects of N doping of TiO_2 (SX) on the photocatalytic decomposition of C_2H_5OH. 1% Au/TiO_2 (A) and 1% Au/TiO_2 + N (B).

Fig. 9 depicts the photocatalytic effects of Au deposited on pure and N-modified TiO_2 (SX). The photoactivity of the N-modified catalysts is seen to be markedly higher than that of Au/TiO_2 free of nitrogen. This is reflected in the conversion of C_2H_5OH and in the amounts of the products formed. The amount of H_2 generated increased by a factor of 6. The effects of N-doping of TiO_2 (SX) were also investigated in visible light. Whereas Au/TiO_2 exhibited relatively little activity, the photoactivity of Au/TiO_2 + N (SX) was clearly higher (Fig. 10).

Some experiments were also devoted to the thermal decomposition of C_2H_5OH on the Au/TiO_2 (Aurolite) catalyst. At 323 K, merely very slight reaction was detected (<1% in 60 min). A more considerable degree of decomposition (~3% in 60 min) was observed at 448 K. The results of these control experiments led us to exclude the contribution of thermal effects to the decomposition of C_2H_5OH induced by illumination.

The effects of illumination on the decomposition of C_2H_5OH can be described analogously as in the case of CH_3OH. The first step is the activation of C_2H_5O involving the donation of a photoelectron formed in the photo-excitation process to this surface species:

$$C_2H_5O_{(a)} + e^- = C_2H_5O_{(a)}{}^{\delta-} \quad (15)$$

This step is followed by the photo-induced decomposition of C_2H_5O to CH_3CHO and H_2:

$$C_2H_5O_{(a)}{}^{\delta-} = CH_3CHO_{(a)}{}^{\delta-} + H_{(a)} \quad (16)$$

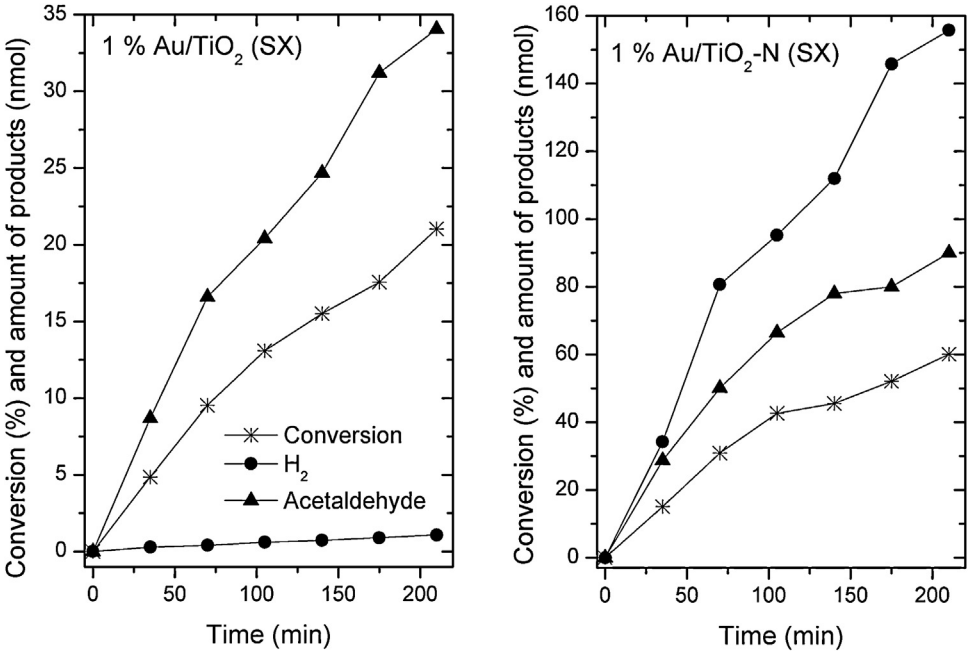

Fig. 10. Effects of N doping of TiO_2 (SX) on the photocatalytic decomposition of C_2H_5OH in the visible light. 1% Au/TiO_2 (A) and 1% Au/TiO_2 + N (B).

The level of photolysis on pure TiO_2 was low, most likely because of the ready recombination between electrons and holes generated by light. The presence of Au on TiO_2, however, markedly enhanced the photocatalytic performance of TiO_2. After the complete conversion of C_2H_5OH, the photocatalyzed decomposition of CH_3CHO came into prominence

$$CH_3CHO_{(a)}{}^{\delta-} = CH_4 + CO_{(a)}{}^{\delta-} \quad (17)$$

$$CO_{(a)}{}^{\delta-} + h^+ = CO_{(g)} \quad (18)$$

The promoting effect of Au appears to be the same as that discussed for the photocatalytic decomposition of CH_3OH. It should be borne in mind that nanosized Au is an active catalyst for the thermal decomposition of C_2H_5OH at elevated temperature [19–23]. This is attributed to promotion of the rupture of a C—H bond in the C_2H_5O species adsorbed on the Au or at the Au/TiO_2 interface.

4. Conclusions

(i) IR spectroscopic studies revealed that the illumination of pure or Au-containing TiO_2 promotes the dissociation of CH_3OH and C_2H_5OH to CH_3O and C_2H_5O species.
(ii) Nanosized Au particles markedly enhance the photocatalytic decompositions of both CH_3OH and C_2H_5OH.
(iii) Besides the production of CO and H_2, $HCOOCH_3$ is formed from CH_3OH and CH_3CHO is formed from C_2H_5OH.
(iv) Through the addition of H_2O or O_2 to these alcohols, the quantity of CO released can be significantly decreased and even completely eliminated in the photodecomposition of CH_3OH.
(v) Lowering the bandgap of TiO_2 by N incorporation increases the photoactivity of the Au/TiO_2 catalyst and leads to the photodecomposition of CH_3OH and of C_2H_5OH even in visible light.

Acknowledgements

This work was supported by the grant OTKA under contract number K 81517 and TÁMOP under contract numbers 4.2.2/B-10/1-2010-0012 and 4.2.2.A-11/1/KONV-2012-0047. The authors express their thanks to Dr. D. Sebők for some spectroscopic experiments. A loan of TiO_2 used for Au/TiO_2 (Aurolite) from STREM Chemicals, Inc. is greatly acknowledged.

References

[1] M. Haruta, T. Kobayashi, H. Sano, N. Yamada, Novel gold catalysts for the oxidation of carbon-monoxide at a temperature far below 0 °C, Chem. Lett. (1987) 405–408.
[2] M. Haruta, N. Yamada, T. Kobayashi, S. Iijima, Gold catalysts prepared by coprecipitation for low-temperature oxidation of hydrogen and of carbon-monoxide, J. Catal. 115 (1989) 301–309.
[3] G.J. Hutchings, Gold catalysis in chemical processing, Catal. Today 72 (2002) 11–17.
[4] G.C. Bond, C. Louis, D.T. Thompson, Catalysis by Gold Catalytic Science Series, Vol. 6, Imperial College Press, London, 2006.
[5] A.S.K. Hashmi, G.J. Hutchings, Gold catalysis, Angew. Chem. Int. Ed. 45 (2006) 7896–7936.
[6] M. Mavrikakis, M.A. Barteau, Oxygenate reaction pathways on transition metal surfaces, J. Mol. Catal. A: Chem. 131 (1998) 135–147.
[7] M. Ojeda, E. Iglesia, Formic acid dehydrogenation on Au-based catalysts at near-ambient temperatures, Angew. Chem. Int. Ed. 48 (2009) 4800–4803.
[8] D.A. Bulushev, S. Beloshapkin, J.R.H. Ross, Hydrogen from formic acid decomposition over Pd and Au catalysts, Catal. Today 154 (2010) 7–12.
[9] X. Zhou, Y. Huang, W. Xing, C. Liu, J. Liao, T. Lu, High-quality hydrogen from the catalyzed decomposition of formic acid by Pd-Au/C and Pd-Ag/C, Chem. Commun. (2008) 3540–3542.
[10] A. Gazsi, T. Bánsági, F. Solymosi, Decomposition and reforming of formic acid on supported Au catalysts: production of CO-free H_2, J. Phys. Chem. C 115 (2011) 15459–15466.
[11] J.G. Hardy, M.W. Roberts, Mechanism of the catalytic decomposition of methanol on gold filaments, J. Chem. Soc. D: Chem. Commun. (1971) 494–495.
[12] M. Haruta, A. Ueda, S. Tsubota, R.M. Torres Sanchez, Low-temperature catalytic combustion of methanol and its decomposed derivatives over supported gold catalysts, Catal. Today 29 (1996) 443–447.
[13] A. Nuhu, J. Soares, M. Gonzalez-Herrera, A. Watts, G. Hussein, M. Bowker, Methanol oxidation on Au/TiO_2 catalysts, Top. Catal. 44 (2007) 293–297.
[14] F. Boccuzzi, A. Chiorino, M. Manzoli, FTIR study of methanol decomposition on gold catalyst for fuel cells, J. Power Sources 118 (2003) 304–310.
[15] M. Manzoli, A. Chiorino, F. Boccuzzi, Decomposition and combined reforming of methanol to hydrogen: a FTIR and QMS study on Cu and Au catalysts supported on ZnO and TiO_2, Appl. Catal. B: Environ. 57 (2005) 201–209.
[16] A. Gazsi, T. Bánsági, F. Solymosi, Hydrogen formation in the reactions of methanol on supported Au catalysts, Catal. Lett. 131 (2009) 33–41.
[17] I. Mitov, D. Klissurski, C. Minchev, Catalytic decomposition of methanol on Au/Fe(2)O(3) catalysts, C. R. Acad. Bulg. Sci. 61 (2008) 1003–1006.
[18] S. Pongstabodee, S. Monyanon, A. Luengnaruemitchai, Hydrogen production via methanol steam reforming over Au/CuO, Au/CeO_2, and Au/CuO-CeO_2 catalysts prepared by deposition-precipitation, J. Ind. Eng. Chem. 18 (2012) 1272–1279.
[19] P.-Y. Sheng, G.A. Bowmaker, H. Idriss, The Reactions of Ethanol over Au/CeO_2, Appl. Catal. A: Gen. 261 (2004) 171–181.
[20] P.-Y. Sheng, G.A. Bowmaker, H. Idriss, The reactions of ethanol over Au/CeO_2, Appl. Catal. A: Gen. 261 (2004) 171–181.
[21] Y. Guan, E.J.M. Hensen, Ethanol dehydrogenation by gold catalysts: the effect of the gold particle size and the presence of oxygen, Appl. Catal. A: Gen. 361 (2009) 49–56.
[22] Y. Guan, E.J.M. Hensen, Ethanol dehydrogenation by gold catalysts: the effect of the gold particle size and the presence of oxygen, Appl. Catal. A: Gen. 361 (2009) 49–56.
[23] A. Gazsi, A. Koós, T. Bánsági, F. Solymosi, Adsorption and decomposition of ethanol on supported Au catalysts, Catal. Today 160 (2011) 70–78.
[24] A. Gazsi, I. Ugrai, F. Solymosi, Production of hydrogen from dimethyl ether on supported Au catalysts, Appl. Catal. A: Gen. 391 (2011) 360–366.
[25] G.R. Bamwenda, S. Tsubota, T. Nakamura, M. Haruta, Photoassisted hydrogen production from a water-ethanol solution: a comparison of activities of Au-TiO_2 and Pt-TiO_2, J. Photochem. Photobiol. A: Chem. 89 (1995) 177–189.
[26] M. Bowker, L. Millard, J. Greaves, D. James, J. Soares, Photocatalysis by Au nanoparticles: reforming of methanol, Gold Bulletin 37 (2004) 170–173.
[27] G. Wu, T. Chen, W. Su, G. Zhou, X. Zong, Z. Lei, C. Li, H_2 production with ultra-low CO selectivity via photocatalytic reforming of methanol on Au/TiO_2 catalyst, Int. J. Hydrogen Energy 33 (2008) 1243–1251.
[28] G. Wu, T. Chen, W. Su, G. Zhou, X. Zong, Z. Lei, C. Li, H_2 production with ultra-low CO selectivity via photocatalytic reforming of methanol on Au/TiO_2 catalyst, Int. J. Hydrogen Energy 33 (2008) 1243–1251.
[29] M. Murdoch, G.I.N. Waterhouse, M.A. Nadeem, J.B. Metson, M.A. Keane, R.F. Howe, J. Llorca, H. Idriss, The effect of gold loading and particle size on photocatalytic hydrogen production from ethanol over Au/TiO_2 nanoparticles, Nature Chemistry 3 (2011) 489–492.
[30] Gy. Halasi, G. Schubert, F. Solymosi, Comparative study on the photocatalytic decomposition of methanol on TiO_2 modified by N and promoted by metals, J. Catal. 294 (2012) 199–206.
[31] Gy. Halasi, G. Schubert, F. Solymosi, Photodecomposition of formic acid on N-doped and metal-promoted TiO_2. Production of CO-free H_2, J. Phys. Chem. C 116 (2012) 15396–15405.
[32] A. Gazsi, G. Schubert, P. Pusztai, F. Solymosi, Photocatalytic decomposition of formic acid and methyl formate on TiO_2 doped with N and promoted with Au. Production of H_2, Int. J. Hydrogen Energy 38 (2013) 7756–7766.
[33] J.-H. Xu, W.-L. Dai, J. Li, Y. Cao, H. Li, H. He, K. Fan, Simple fabrication of thermally stable apertured N-doped TiO_2 microtubes as a highly efficient photocatalyst under visible light irradiation, Catal. Commun. 9 (2008) 146–152.
[34] R. Beranek, H. Kisch, Tuning the optical and photoelectrochemical properties of surface modified TiO_2, Photochem. Photobiol. Sci. 7 (2008) 40–48.
[35] Gy. Halasi, I. Ugrai, F. Solymosi, Photocatalytic decomposition of ethanol on TiO_2 modified by N and promoted by metals, J. Catal. 281 (2011) 309–317.
[36] P. Forzatti, E. Tronconi, G. Busca, P. Tittarelli, Oxidation of methanol to methyl formate over V-Ti oxide catalysts, Catal. Today 1 (1987) 209–218.
[37] G. Jenner, Homogeneous catalytic reactions involving methyl formate, Appl. Catal. A: Gen. 121 (1995) 25–44.
[38] J. Araña, J.M. Doña-Rodríguez, C. Garriga, O. González-Díaz, J.A. Herrera-Melián, J. Pérez, FTIR study of gas-phase alcohols photocatalytic degradation with TiO_2 and AC-TiO_2, Appl. Catal. B: Environ. 53 (2004) 221–232.
[39] W.-C. Wu, C.-C. Chuang, J.-L. Lin, Bonding geometry and reactivity of methoxy and ethoxy groups adsorbed on powdered TiO_2, J. Phys. Chem. B 104 (2000) 8719–8724.
[40] G.L. Chiarello, M.H. Aguirre, E. Selli, Hydrogen production by photocatalytic steam reforming of methanol on noble metal-modified TiO_2, J. Catal. 273 (2010) 182–190.
[41] H. Kominami, H. Sugahara, K. Hashimoto, Photocatalytic selective oxidation of methanol to methyl formate in gas phase over titanium(IV) oxide in a flow-type reactor, Catal. Commun. 11 (2010) 426–429.
[42] K.R. Phillips, S.C. Jensen, M. Baron, S.-C. Li, C.M. Friend, Sequential photooxidation of methanol to methyl formate on TiO_2(1 1 0), J. Am. Chem. Soc. 135 (2013) 574–577.
[43] M.R. Hoffmann, S.T. Martin, W. Choi, D.W. Bahnemann, Environmental applications of semiconductor photocatalysis, Chem. Rev. 95 (1995) 69–96.
[44] A. Linsebigler, G. Lu, J.T. Yates Jr., Photocatalysis on TiO_2 surfaces: principles, mechanisms, and selected results, Chem. Rev. 95 (1995) 735–758.

[45] Z.G. Szabó, F. Solymosi, Influence of the defect structure of support on the activity of catalyst, Actes Congr. Intern. Catalyse 2e Paris 2 (1961) 1627–1651.
[46] F. Solymosi, Importance of the electric properties of supports in the carrier effect, Catal. Rev. 1 (1968) 233–255.
[47] A.A. Ismail, D.W. Bahnemann, I. Bannat, M. Wark, Gold nanoparticles on mesoporous interparticle networks of titanium dioxide nanocrystals for enhanced photonic efficiencies, J. Phys. Chem. C 113 (2009) 7429–7435.
[48] M. Alvaro, B. Cojocaru, A.A. Ismail, N. Petrea, B. Ferrer, F.A. Harraz, V.I. Parvulescu, H. Garcia, Visible-light photocatalytic activity of gold nanoparticles supported on template-synthesized mesoporous titania for the decontamination of the chemical warfare agent Soman, Appl. Catal. B: Environ. 99 (2010) 191–197.